Revisiting the CLBlood Model: Formulation Enhancements and Online Deployment

Spencer R. Van Leeuwen, Gladimir V. G. Baranoski and Bradley W. Kimmel

Natural Phenomena Simulation Group, David R. Cheriton School of Computer Science, University of Waterloo
Technical Report CS-2017-01
February, 2017

Abstract

CLBlood is a cell-based light interaction model for human blood previously developed by the Natural Phenomena Simulation Group (NPSG) at the University of Waterloo. In this report, we revisit several elements of its formulation and describe appropriate enhancements. Furthermore, we compare our current and previous results to demonstrate that the predictive capabilities of our model have been fully preserved in its revised version. We also showcase the online deployment of CLBlood.

I. Introduction

In previous papers [1], [2], we described our cell-based light interaction model for human blood (CLBlood). Since then, we have made several improvements to the model and deployed it online. The improvements we made consist of fixes in the code and changes in the formulation of the model. Although we attempt to provide a self-contained discussion of CLBlood in this document, we note that it is an extension of the previous papers and not a replacement. Therefore, readers looking to understand the entirety of the model should first read the original publication [1] and its accompanying technical report [2].

This document is structured as follows. In Section II, we concisely review the main characteristics of the CLBlood model relevant for the technical discussions presented in this document. In Section III, we outline our improvements to the formulation of the model. In Section IV, we revisit and update the parameters for our *in silico* reproduction of the experiments originally used in CLBlood's evaluation. In Section V, we discuss the online deployment of our model. In Section VI, we compare our current results against the originally published results [1], demonstrating the correctness of our model as previously claimed. In Section VII, we summarize the main contributions of this work and outline potential future improvements to the CLBlood model.

We also include appendices to amend our previous exposition of the model [1], [2]. In particular, the content discussed in the appendices does not affect our implementation of the model, only how it was described in the previous papers. Appendix A contains an updated formulation of the rolling case for red blood cells discussed in Appendix B of our previous technical report [2]. In Appendix B of this report, we discuss additional corrections to our original publication [1] and its accompanying technical report [2].

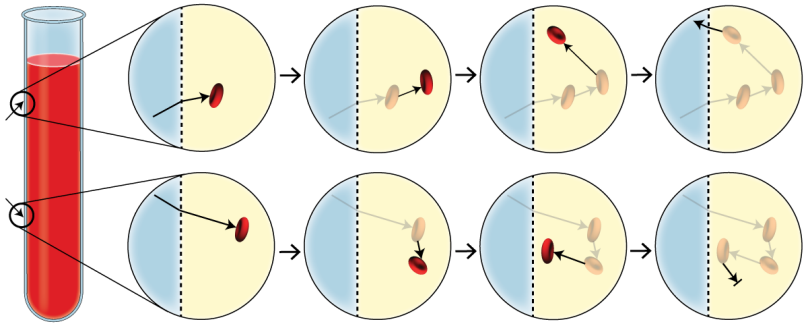

Fig. 1. Depiction of probabilistic, on-the-fly generation of RBCs.

II. CLBlood Overview

As mentioned in the previous section, CLBlood is a cell-based model for the interaction of light with human blood. In particular, it simulates how light interacts with plasma and red blood cells (RBCs) using a first-principles approach. We begin by precomputing the interaction of light with a single RBC and storing the absorption probability in a table. We

then proceed to simulate the interaction of light with the entire blood sample. As light traverses the sample, RBCs are generated probabilistically, on-the-fly as depicted in Fig. 1. The generation of the RBCs is dependent on the distribution of their orientation and the fraction of the sample volume that they occupy, known as hematocrit or HCT. As light hits each RBC, it is either reflected using Fresnel's formulas [3], absorbed using the precomputed absorption table, or transmitted and scattered using the scattering function described in Section III-C.

It has been observed in samples with high hematocrit levels ($HCT > 0.4$) that the orientation of the RBCs is predominantly random, rolling or aligned with the flow at low, intermediate and high shear rates, respectively [4]. In CLBlood, distinct rheological states of a given sample are taken into account by emulating different shear rates using an aggregate distribution of random, rolling and aligned, where the weight for each distribution is a parameter for the model. It has also been observed that at lower hematocrit levels ($HCT < 0.4$), the alignment of RBCs with the flow becomes less pronounced [4]. This fact should be kept in mind when deciding the parameters for a given simulation.

III. Formulation Enhancements

In this section, we extend the formulation of CLBlood by discussing elements that were only mentioned in passing in the previous publication [1].

A RBC is said to hemolyse when its membrane is ruptured. When hemolysis occurs in a whole blood sample, the hemoglobin solution released by the hemolysed RBCs mixes with the plasma, changing the refractive and absorptive properties of the plasma. In this section, we outline how to calculate the new refractive index and absorption coefficient of the plasma, taking into account this mixture of two solutions. Additionally, we discuss the function we use to scatter light being transmitted by a RBC.

A. Refractive Index

When calculating the refractive index (RI) of plasma, we need to account for any hemoglobin that is present as a result of hemolysis. To calculate the resulting RI, $\eta_{result}(\lambda)$, we take a weighted sum of the RIs for the hemoglobin solution contained in RBCs, $\eta_{hemoglobin}(\lambda)$, and plasma, $\eta_{plasma}(\lambda)$. The RI data used for plasma and the hemoglobin solution can be found on our website [5]. In Table I, we present each component's volume fraction of the whole blood sample. However, since the intact RBCs do not contribute to the RI of the resulting medium, we need to rebalance the volume fractions when calculating $\eta_{result}(\lambda)$. Therefore, we need to divide the volume fraction of plasma and the hemolysed hemoglobin solution by $1 - HCT + lysed * HCT$, where $lysed$ is the fraction of hemolysed RBCs.

We calculate the resulting RI as follows:

$$\eta_{result}(\lambda) = \frac{1 - HCT}{1 - HCT + lysed * HCT} * \eta_{plasma}(\lambda) + \frac{lysed * HCT}{1 - HCT + lysed * HCT} * \eta_{hemoglobin}(\lambda). \quad (1)$$

TABLE I

Fraction of the volume attributed to each component of the whole blood sample, where $lysed$ is the fraction of RBCs that have hemolysed.

Component	Volume Fraction
RBCs	$(1 - lysed) * HCT$
Plasma	$1 - HCT$
Hemolysed hemoglobin solution	$lysed * HCT$

B. Absorption

In this section, we start by explaining the calculation of the absorptance of the hemoglobin solution inside a RBC. Then we explain how to calculate the absorptance of plasma given that it contains hemoglobin from hemolysed RBCs.

We start with data for the absorption coefficient of plasma $\mu_{a_p}(\lambda)$ and extinction coefficients for each type of hemoglobin: oxyhemoglobin, $\epsilon_{oh}(\lambda)$; deoxyhemoglobin $\epsilon_{dh}(\lambda)$; sulfhemoglobin, $\epsilon_{sh}(\lambda)$; methemoglobin, $\epsilon_{mh}(\lambda)$; and carboxyhemoglobin,

$\epsilon_{ch}(\lambda)$. These values can be found on our website [5]. Now, we can get the extinction coefficient of the hemoglobin solution inside a red blood cell as follows:

$$\epsilon_h(\lambda) = c_{oh}\epsilon_{oh}(\lambda) + c_{dh}\epsilon_{dh}(\lambda) + c_{sh}\epsilon_{sh}(\lambda) + c_{mh}\epsilon_{mh}(\lambda) + c_{ch}\epsilon_{ch}(\lambda). \tag{2}$$

where c_i is the fraction of hemoglobin that is classified as type i. To get the global absorption coefficient of the hemoglobin solution inside a RBC, we first need to calculate the molality of the hemoglobin inside the cell. This is given by:

$$M_h = MCHC * \frac{1}{h_{g/mol}}, \tag{3}$$

where $MCHC$ is the mean cell hemoglobin content and $h_{g/mol}$ is the molar mass of hemoglobin. Then, we can calculate the global absorption coefficient of the hemoglobin solution using the following formula:

$$\mu_{a_h}(\lambda) = \epsilon_h(\lambda) * M_h + \alpha(\lambda), \tag{4}$$

where $\alpha(\lambda)$ is the absorptance of water. This data is also presented on our website [5]

Similar to the calculation in the previous section, we can now take a weighted sum of the absorption coefficients of plasma and the hemoglobin solution to get:

$$\mu_{a_{result}}(\lambda) = \frac{1 - HCT}{1 - HCT + lysed * HCT} * \mu_{a_p}(\lambda) + \frac{lysed * HCT}{1 - HCT + lysed * HCT} * \mu_{a_h}(\lambda). \tag{5}$$

C. Scattering Function

It has been observed that light transmitted by a RBC is scattered with an average angle of 5° [6] and an exponential falloff [7]. Note that the average scattering angle of 5° refers to the polar scattering angle and the azimuthal angle is assumed to be uniformly distributed in $[0, 2\pi]$. Since we are scattering transmitted light, we will sample the polar angle from the range $[0, \pi/2]$.

Starting with uniform random variables u and v, we generate the scattering angles using Algorithm 1. Note that $\pi/36$ radians is equivalent to 5°. The result of the algorithm is a pair of angles, $polar$ and $azimuthal$, that satisfy the aforementioned requirements and can be used to perturb the ray transmitted by a RBC.

Algorithm 1 Procedure employed to sample polar and azimuthal angles using two uniform random variables, u and v. The produced angles can be used to perturb the ray transmitted by a RBC. Note that $\lfloor \cdot \rfloor$ is the floor operator, which rounds a number down to the nearest integer.

u, v uniformly distributed in $(0, 1]$

$polar = -(pi/36) * \log(u);$
$polar = polar/(pi/2) - \lfloor polar/(pi/2) \rfloor * (pi/2);$

$azimuthal = v * 2 * pi;$

IV. Improved Experiment Parameters

A. Angle of Incidence

In the original publication describing CLBlood [1], we reproduced experiments performed by Meinke *et al.* [8]. However, we discovered a bug in our code and correcting it resulted in the inability to reproduce the results presented in the original paper. In particular, regardless of our choice of distribution of the RBCs' orientations, the reflectance was always higher than the results provided by Meinke *et al.* [8].

This lead to the close examination of a paper by Friebel *et al.* [9] with contributions by M. Meinke, M. Friebel and G. Müller, who are also authors of the paper by Meinke *et al.* [8]. In particular, Friebel *et al.* [9] use the same experimental setup as Meinke *et al.* [8], except they disclose that the light entering the spectrophotometer is parallel to the flow. However, in our previous experiments, we assumed that the incident light was perpendicular to the flow. After discovering this, we

added a parameter to our implementation that allows the incident light to enter the sample parallel to the flow.

B. Hemoglobin Concentration

When we originally reproduced the experiments performed by Meinke *et al.* [8], we used the mean cell volume given by the authors, $83\ \mu m^3$, and the mean cell hemoglobin mass for normal adults, $29.5\ pg$, as given by Lewis *et al.* [10]. We used these values to calculate the corresponding $MCHC$ value of $355.5\ g/L$. However, according to Lewis *et al* [10], this value is outside the normal range of $330 \pm 15\ g/L$. Therefore, we use a $MCHC$ of $330\ g/L$ for the *in silico* experiments reproduced in this document.

C. Scattering Proteins

In CLBlood, we consider the presence of the proteins albumin, globulin and fibrinogen in the plasma and allow their concentration to vary. In particular, these proteins affect the RI of the plasma and can cause Rayleigh scattering as light traverses the plasma. However, we have noticed that changing the concentration of these proteins in the model has a negligible effect on the overall reflectance and scattering of the whole blood sample. Therefore, we have decided to use the average concentration for each protein [11], shown in Table II, by default in our experiments.

TABLE II
AVERAGE CONCENTRATION FOR PROTEINS PRESENT IN PLASMA [11].

Protein	Concentration (g/dL)
Albumin	4.6
Globulin	2.6
Fibrinogen	0.38

V. ONLINE MODEL

For reproducibility and the convenience of other researchers, we have deployed an online interface for CLBlood (Fig. 2) on our webpage [12]. The online interface allows a user to select parameters and run the model. Several precomputation tables can be selected via a dropdown menu allowing researchers to reproduce our published results.

The light interaction models developed by our group are deployed online [13] using our own custom framework, NPSG Distributed (NPSGD) [14], which handles user input to the model and presents results to the user. First, NPSGD generates a user interface on the webpage so that the user can submit a job with their desired parameters. Next, the user is sent a confirmation email which contains a link to start the simulation. Once the model has generated the results, they are formatted and emailed to the user.

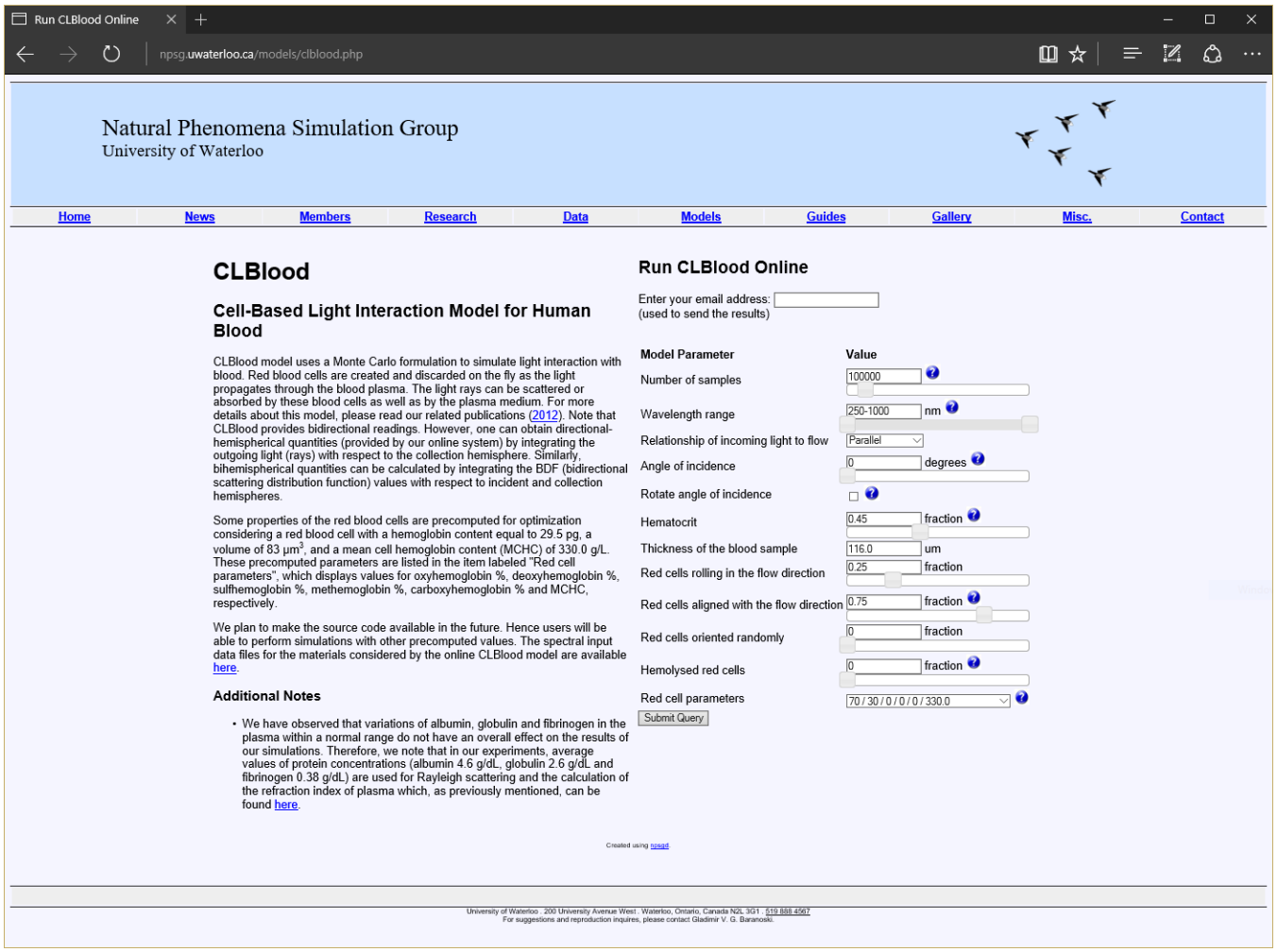

Fig. 2. Online user interface for CLBlood [12].

VI. Experiment Reproduction

In this section, we demonstrate that despite our changes in the model and the parameters for experiment reproduction, the current version of the CLBlood model is capable of reproducing the experiments originally used in its evaluation.

In Fig. 3, we present the results of our *in silico* reproduction of the experiments by Meinke *et al.* [8] using the parameters listed in Table III. In these experiments, the distribution of the RBCs' orientations is a combination of rolling and aligned with the flow. Specifically, we used an alignment of 10%, 30% and 60% for the sample with 0.084, 0.17 and 0.33 HCT, respectively. Note that the percentage of aligned cells is lower in samples with lower hematocrit, which is the expected behaviour as stated in Section II. However, it is impossible for us to know that we have chosen values that exactly match the actual rheological characteristics of the sample used in the experiments by Meinke *et al.* [8]. Therefore, in Fig. 4, we also provide comparisons demonstrating the effect of altering the alignment by $10°$. We see that small variations in the alignment do not have a large effect on the overall reflectance of the sample. This means that even if the selected values for the alignment do not correspond to an exact match, small changes to these values would still provide curves that agree with the experimental results presented by Meinke *et al.* [8].

Additionally, in the original publication of CLBlood [1], we reproduced the experiments of Hammer *et al.* [15] and Yaroslavsky *et al.* [16] which provided data for whole blood scattering at $514\ nm$ and $633.3\ nm$, respectively. In Fig. 5, we present the results of our *in silico* reproduction of these experiments using the parameters in Table IV. We can observe that our model still produces a matching scattering profile.

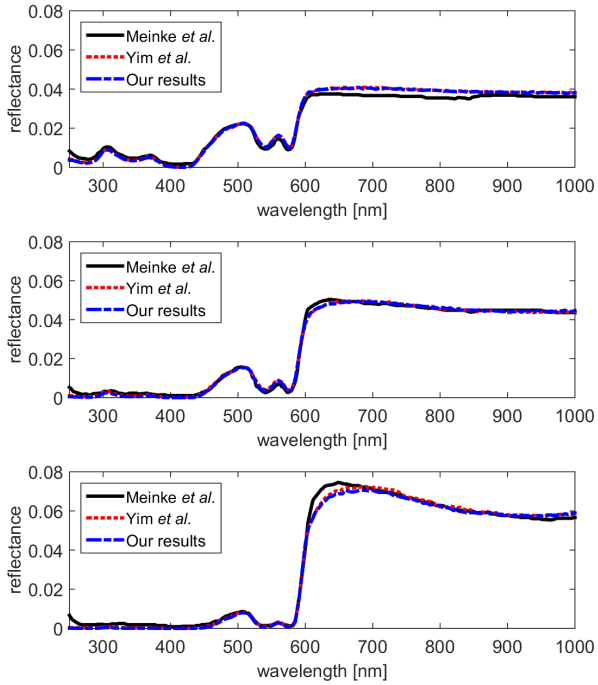

Fig. 3. Results of our *in silico* reproduction of the experiments performed by Meinke *et al.* [8] using the parameters from Table III. They are compared with results from our original implementation of the CLBlood model, by Yim *et al.* [1], and the results presented by Meinke *et al.*. Top: $HCT = 0.084$ and 10% alignment. Middle: $HCT = 0.17$ and 30% alignment. Bottom: $HCT = 0.33$ and 60% alignment.

TABLE III

PARAMETERS FOR THE ONLINE MODEL USED IN OUR REPRODUCTION OF THE EXPERIMENTS PERFORMED BY MEINKE *et al.* [8].

CLBlood Parameter	Value
Number of samples (per wavelength)	1000000
Wavelength range (nm)	250 - 1000
Relationship of incoming light to flow	Parallel
Angle of incidence ($^\circ$)	8
Rotate angle of incidence	False (unchecked)
Hematocrit (fraction)	0.4
Sample thickness (μm)	116.0
Hemolysed cells (fraction)	0.02
Red cell parameters (Oxy-Hb (%) / Deoxy-Hb (%) / Sulf-Hb (%) / Met-Hb (%) / Carboxy-Hb (%) / $MCHC$ (g/L))*	100 / 0 / 0 / 0 / 0 / 330.0

* x-Hb represents the percentage of the hemoglobin in the sample classified as $x$hemoglobin.

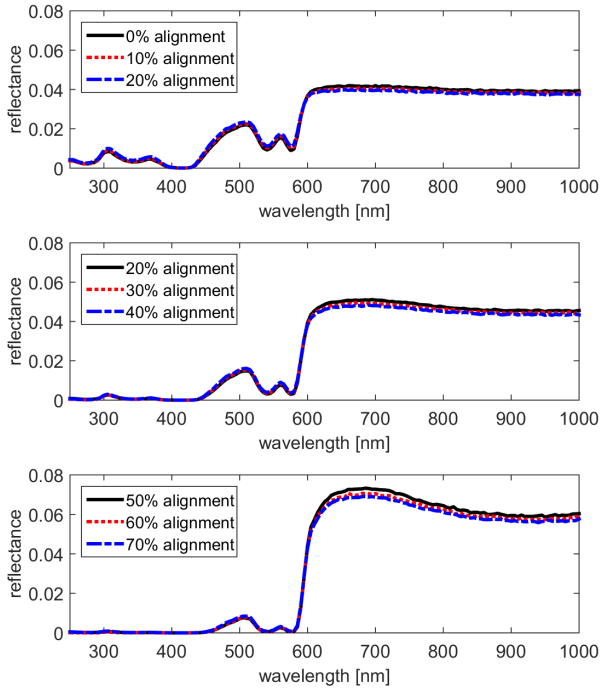

Fig. 4. Results of our *in silico* reproduction of the experiments performed by Meinke *et al.* [8] with varying degrees of alignment using the parameters from Table III. Top: $HCT = 0.084$. Middle: $HCT = 0.17$. Bottom: $HCT = 0.33$.

TABLE IV

PARAMETERS USED IN THE REPRODUCTION OF THE SCATTERING EXPERIMENTS BY HAMMER *et al.* [15] AND YAROSLAVSKY *et al.* [16]. NOTE THAT THE SURROUNDING MEDIUM RI IS CONSTANT ACROSS ALL WAVELENGTHS.

Parameter	Hammer *et al.*	Yaroslavsky *et al.*
Number of samples	10000000	
Wavelength (nm)	514	633.3
Relationship of incoming light to flow	Perpendicular	
Angle of incidence (°)	0	
Hematocrit (fraction)	0.4	0.38
Sample thickness (μm)	120	100
Hemolysed cells (%)	0	
Randomly oriented RBCs (%)	100	
Oxygenation of RBCs (%)	100	
$MCHC$ (g/L)	330.0	
Surrounding medium RI	1.00	1.38

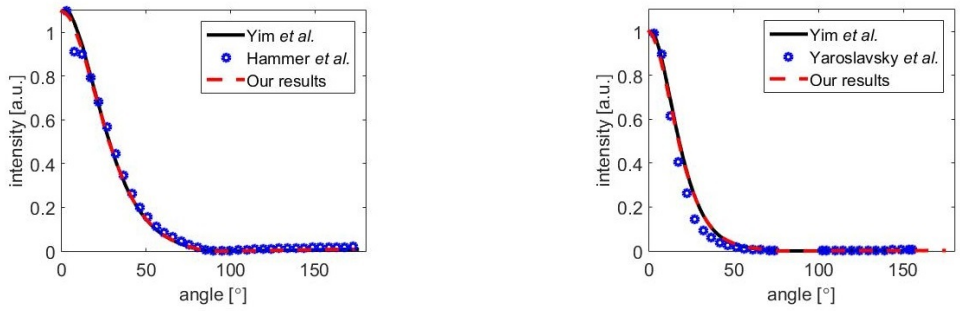

Fig. 5. Results of our *in silico* reproduction of scattering experiments using the parameters from Table IV. They are compared with results from our original implementation of the CLBlood model, by Yim *et al.* [1], and the results presented by Hammer *et al.* (left) and Yaroslavsky *et al.* (right), respectively.

VII. Conclusion

In this report, we have expanded on our previous discussions of the CLBlood model [1], [2] by elaborating on some of its key elements and updating the parameters in experiment reproduction. We also showcased the deployment of the online version of the CLBlood model for the benefit of researchers interested in reproducing our work or employing our model in their own investigations. Finally, we provided quantitative comparisons with the original version of the model [1] and measured results [8], [15], [16]. These comparisons demonstrate the continued predictive capabilities of the model.

The CLBlood model currently depends heavily on the precomputation for the absorption of light by RBCs for faster simulations. However, this makes the model less versatile since we have to run a precomputation every time we want to change the parameters of the RBCs. This also makes the online model less flexible since we need to provide a predetermined list precomputed tables. In the future, it would be useful to implement a version of the CLBlood model that runs on the GPU, similar to our GPU implementation of the ILIT model [17].

References

[1] D. Yim, G. V. G. Baranoski, B. W. Kimmel, T. F. Chen, and E. Miranda, "A cell-based light interaction model for human blood," in *Computer Graphics Forum*, vol. 31, pp. 845–854, Wiley Online Library, 2012.

[2] D. Yim, G. V. G. Baranoski, T. F. Chen, B. W. Kimmel, and E. Miranda, "On the modeling of light interactions with human blood." Technical Report CS-2011-30, School of Computer Science, University of Waterloo, December 2011.

[3] A. S. Glassner, *Principles of Digital Image Synthesis*, vol. 2. Elsevier, 1995.

[4] L.-G. Lindberg and P. A. Oberg, "Optical properties of blood in motion," *Optical Engineering*, vol. 32, no. 2, pp. 253–257, 1993.

[5] NPSG, "Human Blood Data." http://www.npsg.uwaterloo.ca/data/blood.php, February 2017.

[6] P. Latimer, "A wave-optics effect which enhances light absorption by chlorophyll in vivo," *Photochemistry and Photobiology*, vol. 40, no. 2, pp. 193–199, 1984.

[7] M. Kinnunen, A. Kauppila, A. Karmenyan, and R. Myllylä, "Effect of the size and shape of a red blood cell on elastic light scattering properties at the single-cell level," *Biomedical Optics Express*, vol. 2, no. 7, pp. 1803–1814, 2011.

[8] M. Meinke, I. Gersonde, M. Friebel, J. Helfmann, and G. Müller, "Chemometric determination of blood parameters using visible–near-infrared spectra," *Applied Spectroscopy*, vol. 59, no. 6, pp. 826–835, 2005.

[9] M. Friebel, A. Roggan, G. Müller, and M. Meinke, "Determination of optical properties of human blood in the spectral range 250to1100nm using monte carlo simulations with hematocrit-dependent effective scattering phase functions," *Journal of Biomedical Optics*, vol. 11, no. 3, pp. 034021–034021, 2006.

[10] B. J. Bain, I. Bates, M. A. Laffan, and S. M. Lewis, *Dacie and Lewis Practical Haematology*. Elsevier Churchill Livingstone, 11 ed., 2012.

[11] J. M. E Marieb, P Wilhelm, *Human Anatomy*. Pearson Benjamin Cummings, San Francisco, CA, USA, 6 ed., 2011.

[12] NPSG, "Run CLBlood Online." http://www.npsg.uwaterloo.ca/models/clblood.php, February 2017.

[13] NPSG, "Online Models." http://www.npsg.uwaterloo.ca/models.php, February 2017.

[14] G. V. G. Baranoski, T. Dimson, T. F. Chen, B. Kimmel, D. Yim, and E. Miranda, "Rapid dissemination of light transport models on the web," *IEEE Computer Graphics and Applications*, vol. 32, no. 3, pp. 10–15, 2012.

[15] M. Hammer, A. N. Yaroslavsky, and D. Schweitzer, "A scattering phase function for blood with physiological haematocrit," *Physics in Medicine and Biology*, vol. 46, no. 3, p. N65, 2001.

[16] A. N. Yaroslavsky, I. V. Yaroslavsky, T. Goldbach, and H.-J. Schwarzmaier, "Influence of the scattering phase function approximation on the optical properties of blood determined from the integrating sphere measurements," *Journal of Biomedical Optics*, vol. 4, no. 1, pp. 47–53, 1999.

[17] B. Kravchenko, "Balancing fidelity and performance in iridal light transport simulations aimed at interactive applications," Master's thesis, University of Waterloo, 2016.

Appendix A: Explanation of Rolling Case

In Appendix B of our previous technical report for CLBlood [2], we derived $K(\vec{\omega})$, the cross-sectional area of RBCs per unit volume for a ray traveling in the direction $\vec{\omega}$. However, we feel that the rolling case could have been explained better. In this appendix, we will derive $K_{rolling}(\vec{\omega})$ again for clarification.

Let γ_1 and γ_2 be the cross-sectional areas of a RBC viewed from the side and top, respectively. Here, the top is in the direction of the minor axis of the RBC. In Appendix A of the previous report [2], we give the following equation for the cross-sectional area of a RBC:

$$G(\vec{u}, \vec{\omega}) = \gamma_1(1 - \cos\psi) + \gamma_2 \cos\psi, \tag{6}$$

where $\vec{u}$ is the orientation of the cell (i.e., the direction of the top) $\vec{\omega}$ is the direction from which the cell is being viewed, and $\psi \in [0, \pi/2]$ is the angle between $\vec{u}$ and $\vec{\omega}$. To allow for any angle $\psi \in [0, 2\pi]$, we use the following equation for the cross-sectional area:

$$G(\vec{u}, \vec{\omega}) = \gamma_1(1 - |\cos\psi|) + \gamma_2|\cos\psi|. \tag{7}$$

Say that the RBC is rolling (e.g., the motion of a flipping coin) about its local x-axis, $\vec{a}$, by angle θ. Now, the cross-sectional area viewed from the top is no longer constant, but instead a function $\gamma_2'(\theta)$. Furthermore, as the cell rolls, let us fix $\vec{u}$ as the projection of $\vec{\omega}$ onto the plane perpendicular to $\vec{a}$. If $\vec{\omega}$ is parallel to $\vec{a}$, we choose $\vec{u}$ to be an arbitrary vector perpendicular to $\vec{a}$. Note that $\vec{u}$ is no longer the orientation of the RBC. Without loss of generality, we will also say that $\theta = 0$ when $\vec{u}$ is equal to the orientation of the RBC.

Now, we have the following expression:

$$G_{rolling}(\vec{u}, \vec{\omega}) = \gamma_1(1 - |\cos\psi|) + \gamma_2'(\theta)|\cos\psi|. \tag{8}$$

Note that $\gamma_2'(\theta)$ is equal to $G(\vec{u}, \vec{\omega})$, which gives:

$$\gamma_2'(\theta) = \gamma_1(1 - |\cos\theta|) + \gamma_2|\cos\theta|. \tag{9}$$

Substituting (9) into (8), we get:

$$G_{rolling}(\vec{u}, \vec{\omega}) = \gamma_1(1 - |\cos\psi|) + (\gamma_1(1 - |\cos\theta|) + \gamma_2|\cos\theta|)|\cos\psi|. \tag{10}$$

Given the hematocrit of the whole blood sample, HCT, and the volume of each RBC, MCV, the number of cells per unit volume is given by $\delta = HCT/MCV$. Additionally, we use $n(\vec{u})$ to represent the probability density of RBCs with the orientation $\vec{u} \in \Omega$, where Ω is the set of vectors perpendicular to $\vec{a}$. Since the cells are rolling with θ uniformly distributed in $[0, 2\pi]$ and

$$\delta = \int_\Omega n(\vec{u})\,\mathrm{d}\Omega, \tag{11}$$

we get the following:

$$n(\vec{u}) = \frac{\delta}{2\pi}. \tag{12}$$

Finally, the cross-sectional area of RBCs per unit volume is given by:

$$K(\vec{\omega}) = \int_\Omega n(\vec{u})G(\vec{u}, \vec{\omega})\,\mathrm{d}\Omega. \tag{13}$$

By substituting (8) and (12) into (13), we get:

$$K_{rolling}(\vec{\omega}) = \delta\gamma_1(1 - |\cos\psi|) + \frac{\delta}{2\pi}(\gamma_1(2\pi - 4) + 4\gamma_2)|\cos\psi|. \tag{14}$$

A step by step derivation from (13) to (14) can be found in the previous technical report [2].

We can also define $K_{rolling}$ with respect to $\vec{a}$. Let β be the angle between $\vec{a}$ and $\vec{\omega}$. Since we designed $\vec{u}$ such that $\vec{\omega}$ is on the plane determined by $\vec{a}$ and $\vec{u}$, we get $\beta = \pi/2 - \psi$. So $\cos\psi = \sin\beta$. Therefore, $K_{rolling}$ can also be represented as:

$$K_{rolling}(\vec{\omega}) = \delta\gamma_1(1 - |\sin\beta|) + \frac{\delta}{2\pi}(\gamma_1(2\pi - 4) + 4\gamma_2)|\sin\beta|. \tag{15}$$

APPENDIX B: ADDITIONAL CORRECTIONS

In this section, we show some equations that were present in the previous papers [1], [2] and provide corrections. We will not provide context for these equations since a reader interested in this section presumably has access to the previous papers.

In Equation (7) of [1] and [2], we had the following equation:

$$K_{random} = 0.5(\gamma_1 + \gamma_2)\delta. \tag{16}$$

However, we should not be multiplying by 0.5, so the equation should be:

$$K_{random} = (\gamma_1 + \gamma_2)\delta. \tag{17}$$

In Equation (13) of [1] and Equation (15) of [2], we are calculating the absorption coefficient of the hemoglobin solution inside a RBC as follows:

$$\mu_{a_s}(\lambda) = c_f((SaO_2)\epsilon_{oh}(\lambda) + (1 - SaO_2)\epsilon_{dh}(\lambda)) + c_d(\epsilon_{mh}(\lambda) + \epsilon_{ch}(\lambda) + \epsilon_{sh}(\lambda)) + \alpha(\lambda). \tag{18}$$

However, each of the dysfunctional hemoglobin extinction coefficients should be multiplied by a concentration factor such that the factors sum to 1. This is similar to how we multiplied ϵ_{oh} by SaO_2 and ϵ_{dh} by $(1 - SaO_2)$. Alternatively, we could use $\mu_{a_{result}}$ as formulated in this paper (Equations (2), (3) and (4)).